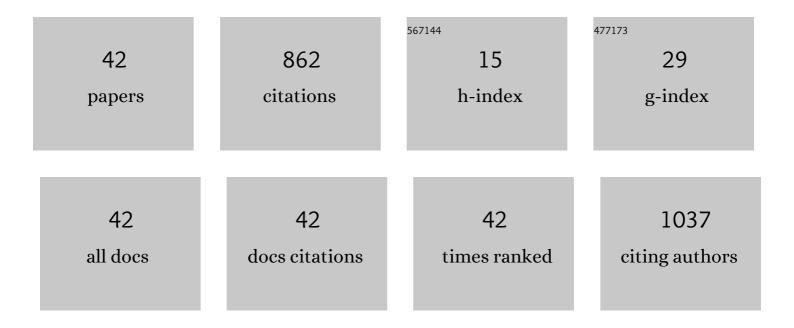
Shuang Jiang

List of Publications by Year in descending order

Source: https://exaly.com/author-pdf/8615653/publications.pdf Version: 2024-02-01



SHUANG HANG

#	Article	IF	CITATIONS
1	Chiral Ceramic Nanoparticles and Peptide Catalysis. Journal of the American Chemical Society, 2017, 139, 13701-13712.	6.6	110
2	Enhanced Water Retention by Using Polymeric Microcapsules to Confer High Proton Conductivity on Membranes at Low Humidity. Advanced Functional Materials, 2011, 21, 971-978.	7.8	96
3	Photocatalytic selective hydroxylation of phenol to dihydroxybenzene by BiOI/TiO2 p-n heterojunction photocatalysts for enhanced photocatalytic activity. Applied Surface Science, 2018, 439, 1047-1056.	3.1	77
4	An ingenious strategy of preparing TiO2/g-C3N4 heterojunction photocatalyst: In situ growth of TiO2 nanocrystals on g-C3N4 nanosheets via impregnation-calcination method. Applied Surface Science, 2018, 433, 963-974.	3.1	71
5	Circular Polarized Light Emission in Chiral Inorganic Nanomaterials. Advanced Materials, 2023, 35, e2108431.	11.1	61
6	Boosted electron-transfer by coupling Ag and Z-scheme heterostructures in CdSe-Ag-WO3-Ag for excellent photocatalytic H2 evolution with simultaneous degradation. Chemical Engineering Journal, 2021, 417, 129298.	6.6	50
7	Ferrocene particles incorporated into Zr-based metal–organic frameworks for selective phenol hydroxylation to dihydroxybenzenes. RSC Advances, 2017, 7, 38691-38698.	1.7	34
8	Controllable synthesis of Ag/AgCl@MIL-88A <i>via in situ</i> growth method for morphology-dependent photocatalytic performance. Journal of Materials Chemistry C, 2019, 7, 5451-5460.	2.7	33
9	Synthesis, characterization, electrochemical properties and catalytic reactivity of N-heterocyclic carbene-containing diiron complexes. RSC Advances, 2015, 5, 29022-29031.	1.7	31
10	A new strategy to achieve enhanced upconverted circularly polarized luminescence in chiral perovskite nanocrystals. Nano Research, 2022, 15, 1047-1053.	5.8	31
11	Synthesis and Characterization of Bio-Inspired Diiron Complexes and Their Catalytic Activity for Direct Hydroxylation of Aromatic Compounds. European Journal of Inorganic Chemistry, 2015, 2015, 817-825.	1.0	30
12	Ligand Exchange Strategy to Achieve Chiral Perovskite Nanocrystals with a High Photoluminescence Quantum Yield and Regulation of the Chiroptical Property. ACS Applied Materials & Interfaces, 2022, 14, 3385-3394.	4.0	25
13	Water-mediated promotion of direct oxidation of benzene over the metal–organic framework HKUST-1. RSC Advances, 2015, 5, 56020-56027.	1.7	16
14	Cu-Deficient plasmonic Cu _{2â^'x} S nanocrystals induced tunable photocatalytic activities. CrystEngComm, 2020, 22, 678-685.	1.3	16
15	Nitrogen heterocyclic carbene containing pentacoordinate iron dicarbonyl as a [Fe]-hydrogenase active site model. Dalton Transactions, 2015, 44, 16708-16712.	1.6	15
16	Polymorphism and molecular conformations of nicosulfuron: structure, properties and desolvation process. CrystEngComm, 2019, 21, 2790-2798.	1.3	15
17	Efficient hydroxylation of aromatic compounds catalyzed by an iron(II) complex with H ₂ O ₂ . Applied Organometallic Chemistry, 2014, 28, 666-672.	1.7	14
18	Controllable self-assembly of BiOI/oxidized mesocarbon microbeads core-shell composites: A novel hierarchical structure facilitated photocatalytic activities. Chemical Engineering Science, 2020, 221, 115653.	1.9	14

SHUANG JIANG

#	Article	IF	CITATIONS
19	Bacitracin-Controlled BiOI/Bi ₅ O ₇ I Nanosheet Assembly and S-Scheme Heterojunction Formation for Enhanced Photocatalytic Performances. ACS Applied Nano Materials, 2022, 5, 6736-6749.	2.4	14
20	Synthesis and properties of novel colorless and thermostable polyimides containing crossâ€linkable bulky tetrafluorostyrol pendant group and organosoluble triphenylmethane backbone structure. Journal of Polymer Science, 2020, 58, 2355-2365.	2.0	13
21	The influence of phosphine ligand substituted [2Fe2S] model complexes as electro-catalyst on proton reduction. RSC Advances, 2018, 8, 42262-42268.	1.7	12
22	Chiroptical Activity of Type II Core/Shell Cu ₂ S/CdSe Nanocrystals. Inorganic Chemistry, 2019, 58, 6534-6543.	1.9	10
23	Synergistic combination of carbon-black and graphene for 3D printable stretchable conductors. Materials Technology, 2020, , 1-10.	1.5	10
24	Versatile solid forms of boscalid: insight into the crystal structures and phase transformations. CrystEngComm, 2019, 21, 6838-6849.	1.3	8
25	Bacitracin-assisted synthesis of spherical BiVO ₄ nanoparticles with C doping for remarkable photocatalytic performance under visible light. CrystEngComm, 2020, 22, 1812-1821.	1.3	8
26	Synthesis, structural characterization, and chemical properties of pentacoordinate model complexes for the active site of [Fe]-hydrogenase. RSC Advances, 2016, 6, 84139-84148.	1.7	7
27	Improved process for 2,3,5-trimethylhydroquinone manufacture: highly efficient catalytic hydrogenation of 2,3,5-trimethylbenzoquinone. Research on Chemical Intermediates, 2015, 41, 663-677.	1.3	5
28	Catalytic Performance and Kinetics of the Precursor of [Fe]-Hydrogenase in the Reaction of Phenol Hydroxylation in Aqueous Phase at Ambient Temperature. Catalysis Letters, 2020, 150, 1238-1243.	1.4	5
29	Chiral 3D CdSe Nanotetrapods. Inorganic Chemistry, 2020, 59, 14382-14388.	1.9	5
30	Bio-inspired Catalyst: [(μ -(SCH(CH2 CH3)CH2 S))Fe(CO)5]2 (μ,k1 ,k1 -DPPF) for Proton Reduction and Phenol Hydroxylation. ChemistrySelect, 2017, 2, 9407-9411.	0.7	4
31	In situ construction of Bi5O7I/Bi4Ti3O12 heterostructure composites with plentiful phase interfaces for the boosted selective oxidation of benzylic alcohols under visible light. Journal of Materials Chemistry C, 0, , .	2.7	4
32	Impact of native achiral ligands on the chirality of enantiopure cysteine stabilized CdSe nanocrystals. Journal of Materials Chemistry C, 2021, 9, 555-561.	2.7	4
33	Effect of the Terminal Ligands of [FeFe]â€Hydrogenase Model Complexes on Proton Reduction Properties and Catalytic Hydroxylation of Benzene. ChemistrySelect, 2017, 2, 3306-3310.	0.7	3
34	Enhanced photothermal behavior derived from controllable self-assembly of Cu _{1.94} S microstructures. Dalton Transactions, 2019, 48, 4495-4503.	1.6	3
35	Effect of α-substitute group on the chirality of monocarboxylic acid stabilized CdSe nanocrystals. Nanotechnology, 2021, 32, 375701.	1.3	3
36	Catalytic reduction of 1,4â€benzoquinone to hydroquinone via [FeFe]â€hydrogenase model complexes under mild conditions. Journal of Chemical Technology and Biotechnology, 2020, 95, 1250-1257.	1.6	2

SHUANG JIANG

#	Article	IF	CITATIONS
37	High selective hydroxylation of phenol catalyzed by PNP ligandâ€containing [FeFe]â€hydrogenase model complexes. Journal of Chemical Technology and Biotechnology, 2020, 95, 2180-2186.	1.6	2
38	Controllable chiral behavior of typeâ€II core/shell quantum dots adjusted by shell thickness and coordinated ligands. Chirality, 2021, 33, 167-175.	1.3	1
39	Synthesis and electrochemical properties of [FeFe]-hydrogenase model complexes with acid-functionalized or base-functionalized ligands. Journal of Applied Electrochemistry, 2017, 47, 583-591.	1.5	Ο
40	The efficient catalytic oxidation of 2,3,6-trimethylphenol with air over composite catalyst to synthesize Vitamin E intermediate. Research on Chemical Intermediates, 2021, 47, 3705-3718.	1.3	0
41	Diphosphine ligandâ€containing model complex of [Fe]â€H 2 ase active site as direct phenol hydroxylation catalyst in the aqueous phase. Journal of Chemical Technology and Biotechnology, 0, , .	1.6	Ο
42	Enhancement of filtration and dispersion properties of Pigment Yellow 14 via an in situ coating strategy onto ethylene–vinyl acetate wax. Research on Chemical Intermediates, 0, , .	1.3	0